Mineralogical Magazine, June 2002, Vol. 66(3), pp. 421–430

Nature and mechanism of ilmenite alteration: a Mössbauer and X-ray diffraction study of oxidized ilmenite from the Beja-Acebuches Ophiolite Complex (SE Portugal)

J. C. WAERENBORGH[1,*], J. FIGUEIRAS[2], A. MATEUS[2] AND M. GONÇALVES[2]

[1] Departamento de Química, Instituto Tecnológico e Nuclear, P-2686-953 Sacavém, Portugal
[2] Departamento de Geologia and CREMINER, Faculdade de Ciências da Universidade de Lisboa, P-1749-016 Lisbon, Portugal

ABSTRACT

Ilmenites from the least-altered rocks of the Beja-Acebuches Ophiolite Complex (SE Portugal), with low Ti values and excess Fe, despite rare optical evidence of hematite exsolution, were studied by ^{57}Fe Mössbauer spectroscopy and X-ray diffraction. According to single-crystal XRD the sequence of alternate layers characteristic of the ideal ilmenite structure is preserved, the excess Fe being accommodated in the Ti layers. No superparamagnetic oxides were detected by ^{57}Fe Mössbauer spectroscopy. The typical spectra of bulk αFe_2O_3 and of Fe^{3+}-containing ilmenite, in the paramagnetic state above 49 K and magnetically ordered at 6 K, are observed. The average degree of oxidation of the ilmenites, estimated from the chemical analysis assuming ideally stoichiometric full cation site occupancies, is also confirmed by ^{57}Fe Mössbauer data. Since our crystal chemistry study gave no evidence of crypto-exsolution textures within the ilmenite with the observed compositions, fast cooling from magmatic temperatures and decomposition of ilmenite in supergene conditions is suggested.

KEYWORDS: ilmenite, Fe-Ti oxides, crystal chemistry, ^{57}Fe Mössbauer spectroscopy, single-crystal X-ray diffraction.

Introduction

THE so-called Beja-Acebuches Ophiolite Complex (BAOC) is a narrow belt of mafic and ultramafic rocks that underlines the southwestern suture of the Variscides in South Portugal and Southwest Spain. Its geological history is characterized by a hot early obduction within the orogen evolution, followed by orogenic climactic deformation and metamorphism and by late metasomatism associated with the shear zones developed in the meantime. A general study on the post-emplacement evolution of the ophiolite sequence and the suture in which it occurs, based on structural, petrographic and chemical data collected at or near these shear zones, has been presented recently (Figueiras *et al.*, 2002).

* E-mail: jcarlos@itn1.itn.pt
DOI: 10.1180/0026461026630038

The BAOC rocks contain trace amounts of oxide minerals. The prevailing primary oxide minerals in ultramafic and primitive mafic rocks of this complex are Cr-bearing spinels while in the metagabbroic rocks they are ilmenite and magnetite, usually occurring as interstitial anhedral grains. Comprehensive characterization of these primary oxides is useful, since a wealth of petrogenetic information pertaining to the igneous, subsolidus and even geodynamic evolution of the oxide-bearing rocks can be deduced from their chemical composition, zonation and/or instability (*c.f.* Belkasmi *et al.*, 2000; Mordberg *et al.*, 2001). Moreover, as there is no metallogenetic evaluation of the BAOC, the study of the oxide minerals may yield useful data for designing adequate mineral exploration surveys.

Besides the alteration associated with orogenic serpentinization and shear-zone-induced metasomatism, BAOC rocks show extensive evidence of

widespread supergene alteration. This is due to the subdued relief of the region which favoured the late Cenozoic development of thick (10s of m) alteration profiles which remain preserved. When clearly present, this supergene alteration is characterized by decomposition of endogenous primary minerals and by deposition of iron oxides and hydroxides. However, there are many indications that even seemingly unaltered rocks are affected by this Late Cenozoic alteration, ilmenite being one of the most affected minerals. As BAOC ilmenite is V-bearing and economic concentrations of the mineral cannot be ruled out entirely, a detailed crystal-chemical study of ilmenite from unaltered metagabbroic rocks was undertaken to determine the extent of cryptic ilmenite alteration and to characterize ilmenite and its alteration products.

In the present work a combined X-ray diffraction (XRD) and ^{57}Fe Mössbauer spectroscopy study of a sample (AZM13) collected at Moinho dos Machadinhos (Serpa, SE Portugal) is reported. Moinho dos Machadinhos, where the BAOC is well exposed and deeply eroded by the Guadiana River, was chosen for its lack of metasomatic alteration and weathering.

Experimental

Mineral chemical analyses were conducted on polished thin-sections using a three-channel wavelength dispersive JEOL-JCXA 733 electron microprobe, operated at an accelerating voltage of 18 kV and a beam current of 25 nA. Natural mineral and pure metal (Cr and V) standards were used before, during and after each analytical session. The estimated error in the values obtained is <2%.

The sample was crushed carefully in a cylindrical rock-crusher, sieved to separate resulting grains by size, and washed in distilled water. The presence of a large number of Fe-containing phases may seriously hinder the analysis of the Mössbauer spectra. When both hematite and magnetite are present, it is difficult to characterize these oxides even if the whole 297–6 K temperature range is scanned. Two fractions of the studied sample were therefore obtained by magnetic separation. The $63 < \phi < 90$ μm size-fraction was passed through a Franz isodynamic separator to extract two magnetic fractions at electric current intensities of 0.02 and 0.2 A, designated AZM13HM and AZM13LM respectively. The non-magnetic fraction under both current intensities was discarded. The number of grains in the AZM13HM fraction was significantly smaller than that in the AZM13LM fraction.

Approximately equant grains were selected under a stereo microscope for their shiny pitchy lustre and conchoidal fracture from the AZM13 sample, and were glued on top of glass fibres and transferred to a goniometer head mounted on an Enraf Nonius CAD-4 diffractometer. Diffracted X-ray intensities were collected at room temperature using an ω-2θ scan mode and graphite-monochromatized Mo-$K\alpha$ radiation (λ = 0.71069 Å). Scans were performed through reciprocal space to find and centre reflections. For most of the grains, only very few reflections were measured which were wide and could not be indexed as a single phase, suggesting an advanced degree of alteration of the primary mineral. Diffracted X-ray intensities were collected for one of the grains which gave well-defined reflections. All of them could be indexed in a rombohedral space-group.

Aliquots of the AZM13HM and AZM13LM magnetic fractions were powdered in an agate mortar. Thin uniform layers of these powders were spread on a glass plate. X-ray diffraction (XRD) patterns of these powders were obtained using a Philips PW1710 powder diffractometer with Cu-$K\alpha$ radiation, a curved graphite crystal monochromator and a PW1820 Bragg-Brentano goniometer.

^{57}Fe Mössbauer spectra of both the AZM13HM and AZM13LM powdered samples were carried out in transmission mode using a conventional constant-acceleration spectrometer and a 25 mCi ^{57}Co source in Rh matrix. The velocity scale was calibrated using an α-Fe foil at room temperature. Spectra were obtained between 297 and 5 K. Low-temperature measurements were performed using a liquid nitrogen/liquid He flow cryostat. Absorbers were prepared by pressing the sample powders ($\approx$5 mg of natural Fe/cm^2) into perspex holders. The spectra were fitted to Lorentzian peaks using a non-linear least-squares computer method (Waerenborgh *et al.*, 1994). The widths and relative areas of both peaks in each quadrupole doublet and of peaks 1-6, 2-5 and 3-4 in each magnetic sextet were constrained to remain equal.

Discussion and results

Microprobe analysis

Table 1 presents representative chemical analytical data obtained for five AZM13 grains. These

data show the presence of Fe,Ti oxide grains with an Fe/Ti atomic ratio varying from 1 up to 1.37 indicating varying degrees of primary ilmenite oxidation. The unit formula estimated for the average composition (Table 1, col. 7) is $Fe^{3+}_{0.22}Fe^{2-}_{0.84}Ti_{0.87}V_{0.043}Mn_{0.017}O_3$, corresponding to an average ratio (Fe^{3-})/(total Fe) ≈ 21%.

Powder diffraction

Phase identification was based on the Mineral Powder Diffraction File Databook (Bayliss *et al.*, 1993). The main mineral phases detected in AZM13LM were ilmenite, hematite, rutile and pseudorutile. Other phases identified were quartz and amphiboles. The strongest peaks of magnetite were also detected. As expected, magnetite, together with ilmenite, were the main phases observed in AZM13HM, although low-intensity diffraction peaks show that all the phases detected in AZM13LM are also present in AZM13HM.

The powder XRD data of AZM13LM were analysed by the Rietveld powder profile program of Young *et al.* (1995) to obtain a rough estimate of the relative molar fractions of ilmenite and hematite. No accurate quantitative mineralogical analysis was attempted since, due to the scarcity of the separate material, it was not possible to prepare adequate samples, i.e. samples with negligible microabsorption and finite-thickness effects. The rough estimation obtained by this method for the ilmenite/hematite molar ratio is Ilm/Hem ≈ 4.

Single-crystal XRD and structure refinement

The unit-cell parameters a_o and c_o (Table 2) were obtained by least-squares refinement of the setting angles of 25 reflections with $28 < 2\theta < 60°$. The measured intensities were corrected for absorption by an empirical method based on ψ scans (North *et al.*, 1968) and for Lorentz-polarization effects (Fair, 1990). The applied absorption correction factors varied between 0.90 and 1.00.

The structure was refined by full-matrix least-squares based on the squares of the structure factors, F^2 (Sheldrick, 1993). The scattering factor for O^{2-} was obtained from Hovestreydt (1983). The scattering factors of the remaining elements and the anomalous dispersion corrections were obtained from Ibers and Hamilton (1974). Scattering factors for fully-ionized species were used in the final refinements because they have always produced a slight improvement in the values of the agreement factors and negligible changes in the estimated values of the adjusted parameters.

Space group $R\bar{3}$ was considered. Extinction was found to be negligible. Neither inconsistent equivalents nor systematic absence violations were observed. Reflections of the type $(h\bar{h}0l)$ with $l = 2n + 1$ were clearly observed, confirming the absence of a *c*-glide plane and indicating that Fe and Ti are not randomly distributed over all the (001) layers. Considering that these ilmenites have ~0.9 Ti oatoms per unit formula, this observation agrees with the results reported for the synthetic $(FeTiO_3)_x$-$(Fe_2O_3)_{1-x}$ solid solutions

TABLE 1. Chemical composition of the studied ilmenites, expressed as the number of cations per 6 oxygens. Elements analysed but not detected are not shown. Columns 1–6 show compositions of individual grains while Column 7 shows the average composition of these grains.

	1	2	3	4	5	6	7
Si	–	–	–	–	–	0.01	–
Ti	1.76	1.70	1.66	1.73	1.58	1.92	1.74
Al	0.00	0.00	0.01	0.00	0.00	0.00	–
V	0.05	0.11	0.10	0.09	0.08	0.08	0.085
Fe^{3+}	0.42	0.49	0.56	0.44	0.76	0.05	0.45
Mg	0.00	0.01	0.00	0.07	0.00	0.00	0.013
Ca	0.00	0.00	0.00	0.00	0.01	0.00	–
Mn	0.04	0.04	0.04	0.02	0.02	0.05	0.035
Fe^{2+}	1.72	1.65	1.61	1.64	1.53	1.87	1.67
Total	4.00	4.00	4.00	4.00	4.00	4.00	4.00

TABLE 2. Crystal data and details of the last stage of crystal structure refinement of an ilmenite single crystal. Chemical composition deduced from the estimated site-occupation factors is $Fe_{1.10(6)}Ti_{0.91(5)}O_3$.

Space Group			$R\bar{3}$ (nr. 148)
Unit-cell parameters (300 K) a_o, c_o			5.070 (1) Å , 14.064 (3) Å
2θ range			2–56°
ω-2θ scan			$\Delta\omega = 1.10 + 0.35 \tan\theta$
Data set			$-6 \leqslant h \leqslant 6$, $-6 \leqslant k \leqslant 6$, $-18 \leqslant l \leqslant 18$
Total data			1002
Unique data			171
Observed data ($F_o \geqslant 4\sigma(F_o)$), n			150
Number of refined parameters, p			20
Final agreement factors			
$R1 = \Sigma\|\|F_o\| - \|F_c\|\|/\Sigma\|F_o\|$			0.0250
$wR2 = \{\Sigma[w(F_o^2 - F_c^2)^2]/\Sigma[w(F_o^2)^2]\}^{1/2}$			0.0758
GoF $= \{\Sigma[w(F_o^2 - F_c^2)^2]/\Sigma w(n-p)\}^{1/2}$			1.119
Site occupations			
(6*c*)	(0, 0, z_1)	Fe	1.01 (5)
(6*c*)	(0, 0, z_2)	Fe	0.09 (4)
		Ti	0.91 (5)
(18*f*)	(x, y, z_3)	O^{2-}	1.00
Position parameters			
6*c*	Fe	(0, 0, z_1)	0.3536 (1)
6*c*	0.91 Ti , 0.09 Fe	(0, 0, z_2)	0.1447 (1)
18*f*	O^{2-}	(x, y, z_3)	0.2963 (5), −0.0200 (5), 0.2542 (2)
Temperature factors (U_{eq})			
(6*c*)	Fe		0.0064 (4) Å^2
(6*c*)	0.91 Ti , 0.09 Fe		0.0085 (4) Å^2
(18*f*)	O^{2-}		0.0086 (5) Å^2

Anisotropic temperature factors expressed as

$$\exp\{-2\pi^2(a^*)^2[(h^2 + k^2 + l^2)U_{11} + 2(hk + hl + kl)U_{12}]\}$$

'Equivalent isotropic temperature factor' $U_{eq} = \frac{1}{3}\sum_{i=1}^{3}\sum_{j=1}^{3} U_{ij}a_i^* a_j^* a_i a_j$

with compositions $x > 0.6$, for which it is not possible to quench-in the high-temperature disordered phases (Harrison *et al.*, 2000).

In the structure of ideal ilmenite, $FeTiO_3$, Fe^{2+} and Ti^{4+} occupy two distinct sets of 6*c* equipositions corresponding to alternate octahedral layers in the hexagonal close-packing sequence of the anions along [001]. In weathered ilmenites, however, some of the Fe is present as Fe^{3+} and some Fe cations are present on the Ti layers and *vice versa* (Murad and Johnston, 1987). Therefore the Fe and Ti site occupation factors were allowed to vary for both 6*c* sites but full-site occupancy was assumed for all positions. Since XRD data is not accurate enough to distinguish between the atomic scattering factors of Fe^{2+} and Fe^{3+}, the final refinements were performed considering only Fe^{2+} and Ti^{4+} scattering factors.

Refinements always converged to full-site occupancy of one of the 6*c* sites by Fe, as expected, and sharing of the other by Fe and Ti. Due to the strong correlation of the site occupation factors with other parameters, namely the temperature factors, there is a large uncertainty in the Fe/Ti atomic ratio on the shared layer. As a result, chemical compositions in the range $Fe_{1.23}Ti_{0.77}O_3$–$Fe_{1.09}Ti_{0.91}O_3$ correspond to agreement factors which are not significantly different. Site occupation factors, s_i, shown in Table 2 are the final values obtained in the refinement procedure, corresponding to the smallest agreement factors. These s_i values

TABLE 3. Number of O^{2-} nearest neighbours (*NN*) and cation–O^{2-} distances, *d*, estimated from the single-crystal XRD refinement of $Fe_{1.10(6)}Ti_{0.91(5)}O_3$.

	NN	Atoms	*d*		*NN*	Atoms	*d*
Fe(6*c*)	3	O^2	2.054(2)	Ti,Fe(6*c*)	3	O^{2-}	1.882(3)
	3	O^2	2.190(3)		3	O^{2-}	2.091(3)

correspond to the unit formula $Fe_{1.10(6)}Ti_{0.91(5)}O_3$. This composition falls within the range of chemical compositions of the set of ilmenite grains studied by microprobe analysis (Table 1).

The estimated unit-cell parameters are intermediate between those of synthetic pure hematite and ilmenite but much closer to those of ilmenite. Variation of c_o between the two solid-solution end-members is approximately linear and much larger than that of a_o (Lindsley, 1976 and Harrison *et al.*, 2000). Therefore c_o is more sensitive to the variation in the Fe/Ti content of the solid solution. The estimated c_o for AZM13 ilmenite corresponds to $Fe_{1.05}Ti_{0.95}O_3$ which is consistent with the refined site occupation factors, considering the estimated standard deviations for the s_i values. Due to the presence of impurity cations in the BAOC ilmenites, however, a perfect match between the dependence of the unit-cell parameters on the ilmenite-hematite mole fraction of the synthetic $(FeTiO_3)_x$-$(Fe_2O_3)_{1-x}$ solid solutions and of the single crystal analysed here should not be expected:

For each 6*c* site there are three short and three long cation–anion distances (Table 3). Considering the O^{2-} radius to be r_O = 1.38 Å, the effective ionic radii from Shannon (1976), 0.605, 0.645 and 0.78 Å, for octahedrally coordinated Ti^{4+}, Fe^{3+} and Fe^{2+}, respectively, correspond to cation–O^{2-} distances, d_i, of 1.985, 2.03 and 2.16 Å. For each 6*c* site, average interatomic distances, $<d>$, may be calculated from these d_i and the estimated site occupation factors, s_i (Table 2) according to:

$$< d > = \Sigma_i d_i s_i$$

If all the Fe on the Fe(6*c*) sites is in the 2+ oxidation state, and on the Fe,Ti(6*c*) sites in the 3+ oxidation state, then $<d>$ = 2.16 Å for the Fe(6*c*) sites and $<d>$ = 1.99 Å for the Fe,Ti(6*c*) sites. These values of $<d>$ fall in between the short and long interatomic distances estimated for the corresponding sites from the refinement of the single-crystal X-ray diffracted intensities (Table 3) confirming the self-consistency of the single-crystal XRD analysis.

^{57}Fe Mössbauer spectroscopy

The spectra of AZM13LM above 49 K (Fig. 1) were fitted by a sextet, due to hematite, and three quadrupole doublets, two due to Fe^{2+} and Fe^{3+} in ilmenite and the third one attributed to Fe^{2+} in an amphibole. At 6 K, only the quadrupole doublet due to the amphibole was observed. On the other hand, besides the hematite sextet, a second sextet attributed to magnetically ordered ilmenite was observed (Fig. 1).

Estimated parameters, summarized in Tables 4 and 5, are in good agreement with values published in the literature for hematite (e.g. Bowen *et al.*, 1993) and natural ilmenites, both above and below the magnetic ordering temperature (Grant *et al.*, 1972; Virgo *et al.*, 1988). The quadrupole doublet with isomer shift and quadrupole splitting larger than those of Fe^{2+} in ilmenite, and consistent with the average parameters of Fe^{2+} on the different crystallographic sites in silicates (e.g. Mitra, 1992), was attributed to the amphibole detected by powder XRD. In agreement with these assignments are also the magnetic ordering temperatures deduced from the spectra, namely ilmenite ordering magnetically between 49 and 6 K and the Fe^{2+} in amphibole remaining paramagnetic down to 6 K. Confirming the reliability of the analyses, the relative areas of the subspectra attributed to each of the phases do not change with temperature, within experimental error.

In the hematite present in AZM13LM, no Morin transition is observed (Fig. 1, Table 4); this may be explained by impurity substitution which is common in natural minerals. 10% Al substitution or a much smaller quantity of tetravalent cations, such as 0.3% Ti substitution, is enough to suppress this magnetic transition (Murad and Johnston, 1987).

In agreement with the powder XRD results, the most obvious difference between the room-

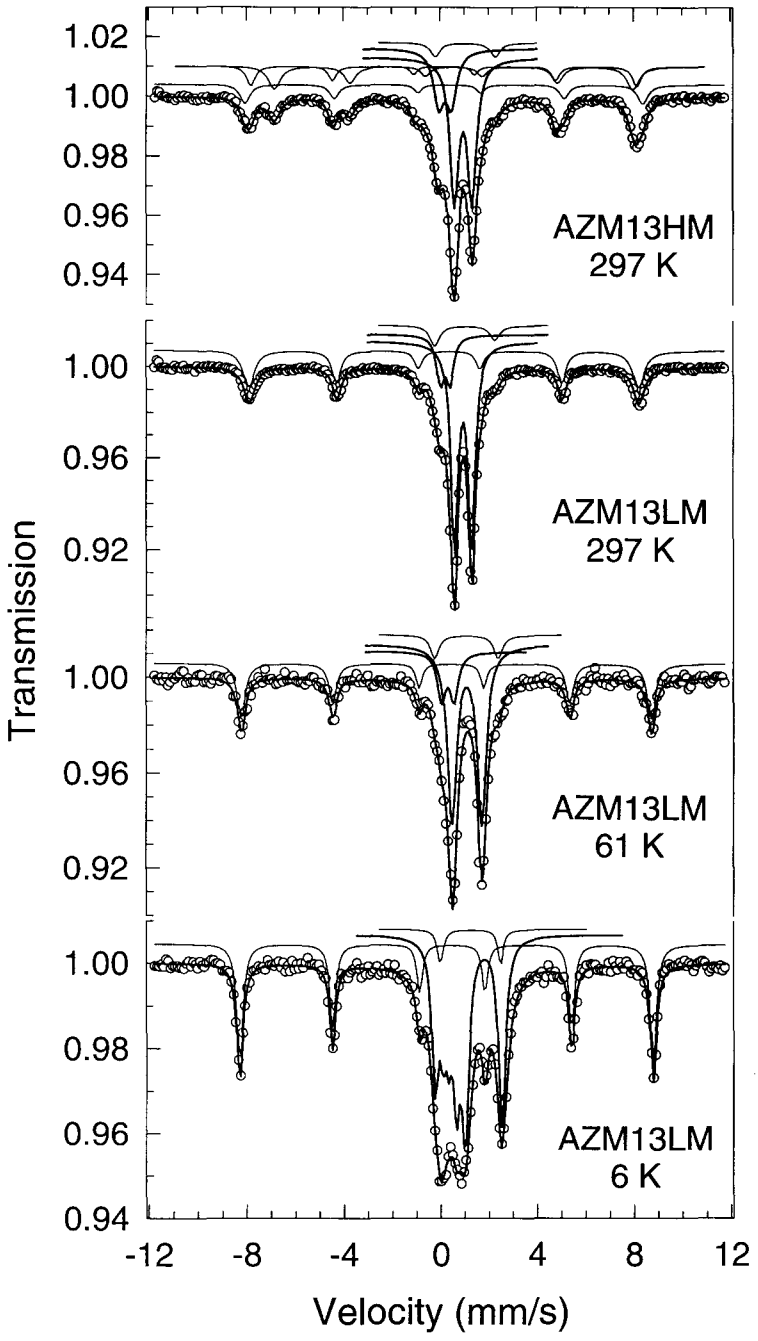

FIG. 1. ^{57}Fe Mössbauer spectra of the AZM13HM and AZM13LM samples at different temperatures. The lines over the experimental points for AZM13LM at $T \geqslant 49$ K are the fits of three doublets and one sextet. The doublets represent Fe^{2+} and Fe^{3+} in ilmenite (thick lines) and Fe^{2+} in amphibole. The sextet represents hematite. In the case of AZM13HM, two additional sextets with lower magnetic splitting, due to magnetite, are also present. For $T = 6$ K the ilmenite contribution to the spectrum is a single sextet (thick line). The doublets and sextets are shown slightly shifted for clarity.

TABLE 4. Parameters estimated from the Mössbauer spectra of AZM13LM taken at different temperatures.

		Hematite Fe^{3+}	Ilmenite Fe^{2+}	Ilmenite Fe^{3+}	Amphibole Fe^{2+}
297 K	δ (mm/s)	0.38	1.06	0.32	1.14
	Δ (mm/s)	–	0.71	0.40	2.49
	ε (mm/s)	−0.22	–	–	–
	B_{hf} (T)	49.9	–	–	–
	Γ (mm/s)	0.38	0.36	0.38	0.47
	I	29%	52%	12%	6%
61 K	δ (mm/s)	0.48	1.21	0.43	1.20
	Δ (mm/s)	–	1.23	0.52	2.63
	ε (mm/s)	−0.20	–	–	–
	B_{hf} (T)	52.5	–	–	–
	Γ (mm/s)	0.30	0.46	0.41	0.41
	I	29%	52%	13%	6%
49 K	δ (mm/s)	0.50	1.29	0.43	1.29
	Δ (mm/s)	–	1.27	0.50	2.74
	ε (mm/s)	−0.21	–	–	–
	B_{hf} (T)	52.6	–	–	–
	Γ (mm/s)	0.30	0.46	0.41	0.54
	I	28%	52%	14%	7%

δ: isomer shift relative to metallic Fe at room temperature; Δ: quadrupole splitting measured in the paramagnetic state; $\varepsilon = (e^2V_{ZZ}Q/4)\,(3\cos^2\theta - 1)$ quadrupole shift calculated from $(\phi_1 + \phi_6 - \phi_2 - \phi_5)/2$ where ϕ_n is the shift of the *n*th line of the sextet due to quadrupole coupling; B_{hf}: magnetic hyperfine field. Γ: full-width at half maximum; *I*: relative areas. Estimated standard deviations are <1% for *I*, <0.1 T for B_{hf} and <0.02 mm/s for the other parameters.

temperature spectra of AZM13HM and AZM13LM (Fig. 1, Tables 4,6) was the presence in AZM13HM of two extra magnetic sextets, with parameters typical of slightly oxidized magnetite (e.g. Bowen *et al.*, 1993). The presence of magnetite adds a large number of extra peaks to the Mössbauer spectrum, some of them overlapping those of the other phases, which is reflected in larger uncertainties for the estimated parameters and relative areas.

TABLE 5. Parameters estimated from the Mössbauer spectra of AZM13LM taken at 6 K.

	Hematite Fe^{3+}	Ilmenite Fe^{2+}, Fe^{3+}	Amphibole Fe^{2+}
6 K			
δ (mm/s)	0.49	1.13	1.36
Δ (mm/s)	–	–	2.50
ε (mm/s)	−0.23	1.56	–
B_{hf} (T)	53.0	4.7	–
Γ (mm/s)	0.28	0.37	0.30
I	28%	64%	7%

Parameters as in Table 4. Estimated standard deviations are <1% for *I*, <0.2 T for B_{hf} and <0.02 mm/s for the other parameters.

The Fe^{3+}/(total Fe) ratio in ilmenites deduced from AZM13HM data is ≈ 30±4% (Table 6) while the same ratio, deduced from the spectra taken at different temperatures of AZM13LM, is ≈20±1%. The latter is consistent with the average chemical composition deduced from electron microprobe data (Table 1), which to a first approximation could be taken to reflect the greater accuracy expected from the AZM13LM Mössbauer data. However, a much larger average Fe^{3+}/(total Fe) for ilmenites which appear together with magnetite after magnetic separation would not be surprising. A larger Fe^{3+}/(total Fe) is correlated with larger total Fe concentration (Table 1) and therefore greater magnetic suscept-

TABLE 6. Parameters estimated from the Mössbauer spectra of AZM13HM taken at room temperature.

	Magnetite		Hematite	Ilmenite		Amphibole
	Fe^{3+}	$Fe^{2.5-}$	Fe^{3+}	Fe^{2+}	Fe^{3+}	Fe^{2+}
δ (mm/s)	0.27	0.67	0.38	1.07	0.32	1.15
Δ (mm/s)	-	-	-	0.73	0.52	2.49
ε (mm/s)	0.00	0.00	−0.22	-	-	-
B_{hf} (T)	49.5	46.0	51.0	-	-	-
Γ (mm/s)	0.33	0.46	0.38	0.44	0.52	0.47
I	11%	17%	12%	39%	17%	4%

Parameters as in Table 4. Estimated standard deviations are <2% for I, <0.2 T for B_{hf} and <0.02 mm/s for the other parameters.

ibility. Magnetic separation concentrated the more oxidized ilmenites with magnetite in AZM13HM. The AZM13HM fraction is much smaller than the AZM13LM fraction. Ilmenites in AZM13LM, with lower Fe concentrations, are therefore expected to be representative of the typical AZM13 ilmenites while the Fe-rich ones present in AZM13HM are the more oxidized minority.

The approximate ilmenite/hematite molar ratio Ilm/Hem ≈ 4 deduced from the powder XRD is consistent with the relative areas estimated from the AZM13LM Mössbauer spectra. If 28% of the Fe in the whole sample is in the hematite (α-Fe_2O_3) structure (Tables 4,5), and 64% in the ilmenite with average composition $Fe^{3+}_{0.22}Fe^{2+}_{0.84}Ti_{0.87}V_{0.043}Mn_{0.017}O_3$ (Table 1, column 7), then

$$(1.06 \times \text{Ilm})/(2 \times \text{Hem}) = 0.64/0.28$$

and the Ilm/Hem molar ratio estimated from Mössbauer data is ≈ 4.3.

As shown above, the Fe^{3+}/(total Fe) ratios in ilmenites obtained from Mössbauer data of AZM13LM and from the average chemical composition deduced from the electron microprobe data are the same within experimental error. Ilm/Hem molar ratios in AZM13LM estimated from powder XRD and Mössbauer spectroscopy are also similar if the same average chemical composition is considered. Since microprobe data was obtained from a large number of ilmenite grains the consistency of the above estimated Fe^{3+}/(total Fe) ratios and Ilm/Hem molar ratios argues in favour of the AZM13LM ilmenites being representative of those in the whole AZM13 sample, as already suggested by the relative amounts of AZM13HM and AZM13LM fractions.

Conclusion

The ratio (Fe^{3+})/(total Fe) ≈ 20±2% estimated for AZM13 ilmenites from the ^{57}Fe Mössbauer data is in very good agreement with the average chemical composition deduced from microprobe analyses $Fe^{3+}_{0.22}Fe^{2+}_{0.84}Ti_{0.87}V_{0.043}Mn_{0.017}O_3$ and from the refinement of single-crystal XRD data, $Fe_{1.10(6)}Ti_{0.91(5)}O_3$. The ideally stoichiometric full-site occupancy of the ilmenites present in AZM13 is therefore confirmed.

The single-crystal X-ray refinement further showed that the crystallite measured should have nonequivalent alternate layers of cations as found in ideal ilmenite. These data give no evidence of superstructures in ilmenite due to the periodic intercalation of hematite-like sequences of layers. Instead, the oxidation of ≈20% of the total Fe to Fe^{3+} seems to be achieved by accommodating the excess Fe in the Ti layers, keeping the alternate sequence of layers of the ideal ilmenite structure.

This conclusion, drawn from the single-crystal XRD, is in agreement with the powder XRD and Mössbauer spectroscopy data. According to these techniques, the hematite found in the sample can only correspond to a considerable number of consecutive hematite-like crystallographic planes since well-defined peaks are seen in powder XRD and, according to the Mössbauer effect, the long-range magnetic ordering is already well established at room temperature for all the Fe atoms in this oxide (the relative area of the hematite sextet is the same in the temperature range 300–6 K). There is no evidence of the superparamagnetic behaviour which would have been detected if α-Fe_2O_3 was present in the form of a few hematite-like layers. The slightly lower value

estimated for the magnetic hyperfine field (Tables 4–6) and the absence of the Morin transition, as opposed to the pure oxide, are easily explained by low concentration impurities, namely Ti.

The chemical composition and the lack of hematite exsolution in the ilmenites indicate fast cooling from magmatic temperatures, probably caused by obduction over cold continental crust, as is more thoroughly discussed in Figueiras *et al.* (2002). When the oxidation degree of Fe due to weathering becomes too large, the ilmenite crystal structure seems to break down as also suggested by the large number of polycrystalline and poorly crystallized grains found when attempting to collect single-crystal diffractometric data. Fe is seggregated and forms Ti-containing hematite. Ti-rich phases evolve into pseudorutile and eventually rutile as suggested by the observation of large amounts of these Ti oxides in the powder X-ray diffraction patterns. The structural degradation of many optically fresh-looking ilmenite grains and the XRD detection of optically inconspicuous ilmenite alteration products, indicates that even fresh-looking rocks may have significant weathering and this should be taken into account when evaluating the metallogenetic potential of the BAOC.

Acknowledgements

This work was supported by PRAXIS (Portugal) under contract nr. PBIC/C/CTA/2112/95.

References

Bayliss, P., Erd, R.C., Mrose, M., Roberts, A.C. and Sabina, A.P. (1993) *Mineral Powder Diffraction File Databook*. International Centre for Diffraction Data, Park Lane, Pennsylvania, USA, 774 pp.

Belkasmi, M., Cuney, M., Pollard, P.J. and Bastoul, A. (2000) Chemistry of the Ta-Nb-Sn-W oxide minerals from the Yichun rare metal granite (SE China): genetic implications and comparison with Moroccan and French Hercynian examples. *Mineralogical Magazine*, **64**, 507–523.

Bowen, L.H., De Grave, E. and Vandenberghe, R.E. (1993) Mössbauer effect studies of magnetic soils and sediments. Pp. 115–159 in: *Mössbauer Spectroscopy Applied to Magnetism and Materials Science*, Vol. 1 (G.J. Long and F. Grandjean, editors). Plenum Press, New York.

Fair, C.K. (1990) *MOLEN*. Enraf-Nonius, Delft, The Netherlands.

Figueiras, J., Mateus, A., Gonçalves, M., Waerenborgh, J.C. and Fonseca, P. (2002) Geodynamical evolution of the South Variscan Iberian Suture as recorded by mineral transformations. *Geodynamica Acta*, **15**, 45–61.

Grant, R.W., Housley, R.M. and Geller, S. (1972) Hyperfine interaction of Fe^{2+} in ilmenite. *Physical Review B*, **5**, 1700–1704.

Harrison, R.J., Redfern, S.A.T. and Smith, R.I. (2000) In-situ study of the $R\bar{3}$ to $R\bar{3}c$ phase transition in the ilmenite-hematite solid solution using time-of-flight neutron power diffraction. *American Mineralogist*, **85**, 194–205.

Hovestreydt, E. (1983) On the atomic scattering factor for O^{2-}. *Acta Crystallographica A*, **39**, 268–269.

Ibers, J.A. and Hamilton, W.C. (1974) *International Tables for X-ray Crystallography. Vol. 4. Revised and supplementary tables*. Kynoch Press, Birmingham, England, 854 pp.

Lindsley, D.H. (1976) The crystal chemistry and structure of oxide minerals as exemplified by the Fe-Ti oxides. Pp. L1–L60 in: *Oxide Minerals* (D. Rumble III, editor). Reviews in Mineralogy, **3**, BookCrafters Inc., Chelsea, Michigan, USA.

Mitra, S. (1992) *Applied Mössbauer Spectroscopy. Theory and Practice for Geochemists and Archaelogists*. Pergamon Press, Oxford, UK, 381 pp.

Mordberg, L.E., Stanley, C.J., and Germann, K. (2001) Mineralogy and geochemistry of trace elements in bauxites: The Devonian Schugorsk deposit, Russia. *Mineralogical Magazine*, **65**, 81–101.

Murad, E. and Johnston, J.H. (1987) Iron oxides and hydroxides. Pp. 507–582 in: *Mössbauer Spectroscopy Applied to Inorganic Chemistry* Vol. 2 (G.J. Long, editor). Plenum Press, New York.

North, A.C.T., Phillips, D.C. and Mathews, F.S. (1968) A semi-empirical method of absorption correction. *Acta Crystallographica A*, **24**, 351–359.

Shannon, R.D. (1976) Revised effective ionic radii and systematic studies of interatomic distances in halides and chalcogenides. *Acta Crystallographica A*, **32**, 751–767.

Sheldrick, G.M. (1993) *SHELXL-93: Program for Crystal Structure Refinement*. University of Göttingen, Germany, 109 pp.

Virgo, D., Luth, R.W., Moats, M.A. and Ulmer, G.C. (1988) Constraints on the oxidation of the mantle: an electrochemical and ^{57}Fe Mössbauer study of mantle derived ilmenites. *Geochimica et Cosmochimica Acta*, **52**, 1781–1794.

Waerenborgh, J.C., Figueiredo, M.O., Cabral, J.M.P. and Pereira, L.C.J. (1994) Powder XRD structure refinements and ^{57}Fe Mössbauer effect study of synthetic $Zn_{1-x}Fe_xAl_2O_4$ ($0 < x \leq 1$) spinels annealed at different temperatures. *Physics and Chemistry of Minerals*, **21**, 460–468.

Young, R.A., Sakthivel, A., Moss, T.S. and Paiva-Santos, C.O. (1995) DBWS-9411 – an upgrade of the DBWS programs for Rietveld Refinement with PC and mainframe computers. *Journal of Applied Crystallography*, **28**, 366–367.

[*Manuscript received 30 August 2001: revised 4 April 2002*]